Terahertz imaging through self-mixing in a quantum cascade laser

Paul Dean,[1,*] Yah Leng Lim,[2] Alex Valavanis,[1] Russell Kliese,[2] Milan Nikolić,[2] Suraj P. Khanna,[1] Mohammad Lachab,[1] Dragan Indjin,[1] Zoran Ikonić,[1] Paul Harrison,[1] Aleksandar D. Rakić,[2] Edmund H. Linfield,[1] and A. Giles Davies[1]

[1]*School of Electronic and Electrical Engineering, University of Leeds, Leeds, LS2 9JT, UK*

[2]*The University of Queensland, School of Information Technology and Electrical Engineering, QLD, 4072, Australia*

**Corresponding author: p.dean@leeds.ac.uk*

Received April 13, 2011; revised May 25, 2011; accepted May 31, 2011;
posted May 31, 2011 (Doc. ID 145642); published July 1, 2011

We demonstrate terahertz (THz) frequency imaging using a single quantum cascade laser (QCL) device for both generation and sensing of THz radiation. Detection is achieved by utilizing the effect of self-mixing in the THz QCL, and, specifically, by monitoring perturbations to the voltage across the QCL, induced by light reflected from an external object back into the laser cavity. Self-mixing imaging offers high sensitivity, a potentially fast response, and a simple, compact optical design, and we show that it can be used to obtain high-resolution reflection images of exemplar structures. © 2011 Optical Society of America

OCIS codes: 110.6795, 250.5960, 140.5960, 040.2235.

The quantum cascade laser (QCL) [1,2] is a compact semiconductor source of terahertz (THz) frequency radiation that is potentially well suited for imaging across a broad range of applications. These inter-subband, heterostructure devices are capable of cw emission with powers exceeding 100 mW [3]. Furthermore, narrowband emission has been demonstrated at frequencies from 1.2 to 5.0 THz [4,5], with operating temperatures as high as 186 K being obtained in pulsed mode [6]. The high powers of THz QCLs, coupled with the possibility of tailoring the emission to frequencies that exhibit low atmospheric attenuation, has enabled real-time imaging over stand-off distances exceeding 25 m [5]. Real-time imaging in both transmission and reflection geometries has also been demonstrated at near-video-rates (20 frames per second) through use of a microbolometer focal-plane array [7]. Other detector systems employed for imaging with THz QCLs include room-temperature Schottky diodes [8], Golay cells [9], pyroelectric detectors [10] and cryogenically-cooled bolometers [11]. While room-temperature THz detectors avoid the reliance on cryogenic liquids, their response is typically slow and, with the exception of Schottky diodes, sensitivities are significantly poorer than those achieved with cryogenically cooled bolometric detection.

In this Letter, we demonstrate a THz frequency imaging system that uses a single QCL to both generate and sense the THz radiation through self-mixing, an effect that occurs when the radiation from a laser is reflected from an external target back into the laser cavity [12,13]. The reflected light interferes (mixes) with the intracavity field, producing variations in the threshold gain, emitted power, lasing spectrum, and junction voltage. To date, self-mixing in THz QCLs has been used only to determine the linewidth enhancement factor of the laser [14]. In our scheme, imaging is performed by monitoring perturbations to the voltage dropped across the QCL as a reflective object is scanned through the emitted THz beam. The QCL itself behaves as an interferometric sensor, thereby removing the need for an external detector. We demonstrate high-resolution reflection imaging of exemplar metallic structures, including imaging through visibly opaque screens.

The homodyne (coherent) nature of a self-mixing scheme inherently provides very high-sensitivity detection, potentially at the quantum noise limit, and therefore a high signal-to-noise ratio can be expected in imaging data [15,16]. Furthermore, the maximum speed of response to optical feedback is determined by the frequency of relaxation oscillations in the laser. In the case of THz QCLs, the lifetime of the upper state of the lasing transition is limited by elastic and inelastic scattering mechanisms to a few picoseconds [17,18], enabling response frequencies of the order of 100 GHz. Self-mixing systems also have a simple optical design and offer the advantage of potential implementation into arrays [19].

A schematic diagram of our imaging system is shown in Fig. 1. The THz QCL consisted of a 10-μm-thick GaAs—AlGaAs bound-to-continuum active region [20] that was processed into a semi-insulating surface-plasmon ridge waveguide with dimensions 3 mm × 140 μm. The QCL was mounted on the cold finger of a continuous-flow cryostat fitted with a polythene window and operated in cw mode at a heat sink temperature of 25 K. Measurements of the source emission spectrum for a drive

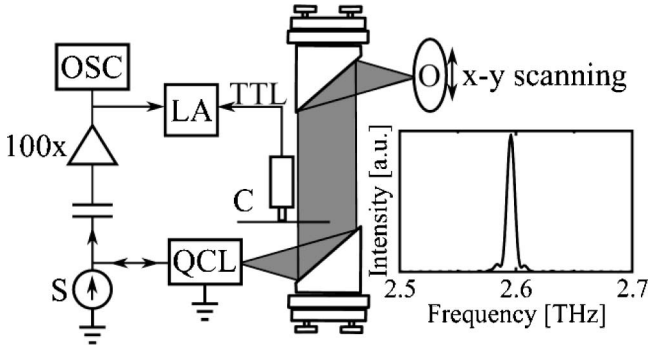

Fig. 1. Schematic diagram of the experimental system used for THz imaging with a QCL. S, current source; OSC, oscilloscope; LA, lock-in amplifier; C, mechanical chopper; O, object. Inset: emission spectrum of the THz QCL, as measured using a Fourier-transform spectrometer.

current of 900 mA, obtained using a Fourier-transform infrared spectrometer with a spectral resolution of 7.5 GHz, indicate emission in a single longitudinal mode at 2.60 THz (inset, Fig. 1). Radiation from the QCL was collimated using a 2 in,$f/2$ off-axis parabolic reflector and focused at normal incidence onto the object, using a second identical reflector. The total optical path between source and object was 65 cm, with ~240 μW of power being incident on the object, as measured using a calibrated THz frequency powermeter. The laser beam was mechanically modulated at a frequency of 215 Hz using an optical chopper and coupled back into the laser cavity along the same optical path as the incident radiation. The self-mixing-induced perturbations to the voltage across the QCL terminals were amplified by an ac-coupled differential amplifier, with a gain of 100. This signal was then measured by a lock-in amplifier and synchronized with the chopper frequency, as well as by being observed directly on an oscilloscope. For image acquisition, the object was raster scanned in two dimensions using a two-axis, computer-controlled translation stage, with the lock-in amplifier output being recorded at each position. No atmospheric purging was employed.

Figure 2(a) shows a typical waveform obtained, after amplification of the ac-coupled voltage across the QCL terminals in response to a modulated feedback signal, for the case in which the object was a reflective metallic plate. The mean junction voltage was 3.1 V, with a driving current of 900 mA. Figure 2(b) shows the rms self-mixing signal measured as a function of the QCL drive current, obtained by positioning a corner cube retroreflector in the collimated portion of the beam. Also shown is the power-current characteristic of the QCL. This demonstrates that the QCL is most sensitive to optical feedback at operating currents near threshold. Similar behavior has been observed previously in junction semiconductor lasers [21]. We estimated the detection limit of our system by inserting attenuators between the QCL and beam focus. Instead of modulating the amplitude of the feedback signal using an optical chopper, for this measurement the reflective plate was attached to a subwoofer speaker that was vibrated at ~20 Hz to generate a time-varying optical path length. This ensured that weak reflections from the attenuators remained constant and made no contribution to the heterodyne signal. We found that our system could tolerate ~48 dB of attenuation, indicating a minimum detectable reflected power equal to ~4 nW.

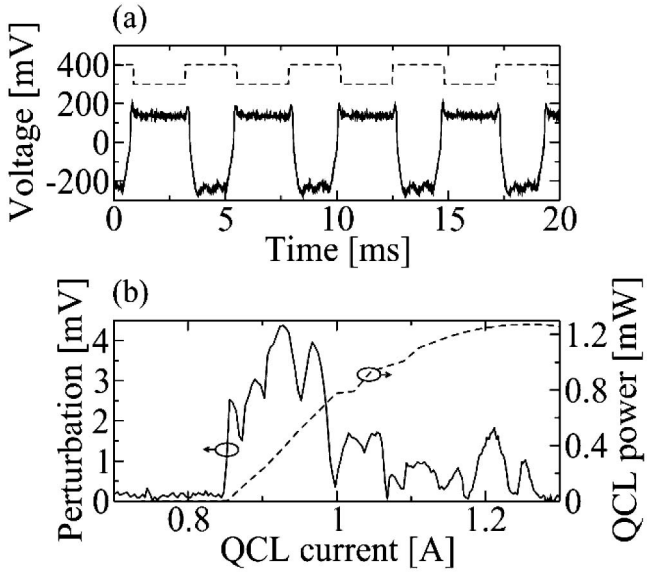

Fig. 2. (a) Exemplar waveform (bottom trace) obtained after amplification of the ac-coupled voltage dropped across the QCL in response to a square-modulated feedback signal. The TTL feedback control signal (top trace) has been scaled and offset. (b) Root-mean-square self-mixing signal (left axis) and QCL power (right axis) as a function of the QCL driving current.

Figure 3(a) shows an image of a scalpel blade obscured by a high-density polyethylene FedEx envelope. The step-size for this image was 250 μm and the lock-in time constant was 5 ms. The magnitude of the self-mixing signal depends on the phase of the field coupled back into the laser cavity, or equivalently the length of the extended cavity formed between the QCL and the sample being imaged. This explains the fringes observed in this image, which represent the surface morphology of the object, with adjacent fringes corresponding to a longitudinal displacement of half a wavelength, or ~58 μm in this case. This demonstrates the potential applicability of this sensing technique to three-dimensional imaging. The modulation transfer function for the system was determined by imaging a set of gold-on-quartz bar resolution targets [10]. By defining the resolution limit at the 20% modulation threshold, Fig. 3(b) shows that our system is capable of resolving features down to widths of 250 μm or lower. This allows high-resolution imaging to be performed, as demonstrated in the exemplar image of a British two-pence coin in Fig. 3(c). For this 25.9 mm× 25.9 mm image (corresponding to 259 pixel × 259 pixel), the shortest acquisition time realizable using our system was 19 minutes.

It should be noted that, in our scheme, the QCL is operated in cw mode in order to achieve good spectral purity. Since the reported scheme is sensitive to the phase of the reflected field, poorer spectral purity would result in reduced detection sensitivity, and would also adversely

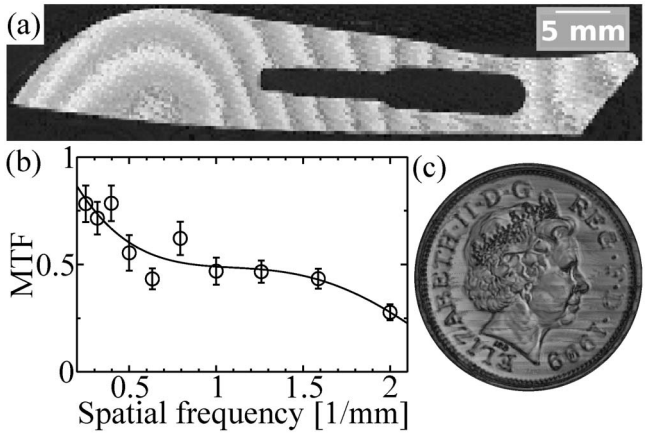

Fig. 3. (a) Exemplar image, obtained using our system, of a scalpel blade obscured behind a high-density polyethylene FedEx envelope. (b) Modulation transfer function of the system, obtained from images of gold-on-quartz bar resolution targets. (c) A high-resolution image of a British two-pence coin (diameter = 25.9 mm).

affect the ability of the system to resolve the morphology of the object accurately [22]. Nevertheless, the QCL could in principle be operated in pulsed mode, thereby removing the need for the mechanical chopper. This would also facilitate faster modulation of the self-mixing signal, which is currently limited by the maximum usable chopper speed.

In summary, we have demonstrated THz imaging using a single QCL as both the source and detector, by monitoring the self-mixing voltage induced across the QCL terminals by optical feedback from an object. This technique is well-suited to fast, high-resolution, high-sensitivity imaging at THz frequencies without the need for an external THz detector.

This project is funded under the European Research Council (ERC) Advanced Grants New Opportunities in Terahertz Engineering and Science (NOTES) and Terahertz Optoelectronics from the Science of Cascades to Applications (TOSCA), and the Innovative Research Call in Explosives and Weapons Detection (2007), a cross-government program, sponsored by a number of government departments and agencies under the counter-terrorism strategy (CONTEST). This research was supported under Australian Research Council's Discovery Projects funding scheme. DP0988072.

References

1. R. Köhler, A. Tredicucci, F. Beltram, H. E. Beere, E. H. Linfield, A. G. Davies, D. A. Ritchie, R. C. Iotti, and F. Rossi, Nature **417**, 156 (2002).
2. B. Williams, Nat. Photon. **1**, 517 (2007).
3. B. Williams, S. Kumar, Q. Hu, and J. L. Reno, Electron. Lett. **42**, 89 (2006).
4. C. Walther, M. Fischer, G. Scalari, R. Terazzi, N. Hoyler, and J. Faist, Appl. Phys. Lett. **91**, 131122 (2007).
5. A. W. M. Lee, Q. Qin, S. Kumar, B. S. Williams, Q. Hu, and J. L. Reno, Appl. Phys. Lett. **89**, 141125 (2006).
6. S. Kumar, Q. Hu, and J. L. Reno, Appl. Phys. Lett. **94**, 131105 (2009).
7. A. W. M. Lee, B. S. Williams, S. Kumar, Q. Hu, and J. L. Reno, IEEE Photon. Technol. Lett. **18**, 1415 (2006).
8. S. Barbieri, J. Alton, C. Baker, T. Lo, H. E. Beere, and D. Ritchie, Opt. Express **13**, 6497 (2005).
9. K. L. Nguyen, M. L. Johns, L. F. Gladden, C. H. Worrall, P. Alexander, H. E. Beere, M. Pepper, D. A. Ritchie, J. Alton, S. Barbieri, and E. H. Linfield, Opt. Express **14**, 2123 (2006).
10. P. Dean, M. U. Shaukat, S. P. Khanna, M. Lachab, A. Burnett, A. G. Davies, E. H. Linfield, and S. Chakraborty, Opt. Express **16**, 5997 (2008).
11. P. Dean, N. K. Saat, S. P. Khanna, M. Salih, A. Burnett, J. Cunningham, E. H. Linfield, and A. G. Davies, Opt. Express **17**, 20631 (2009).
12. T. Bosch, C. Bes, L. Scalise, and G. Plantier, in *Encyclopedia of Sensors*, C. A. Grimes, E. C. Dickey, and M. V. Pishko, eds. (American Scientific, 2006), Vol. X, pp. 1–20.
13. S. Donati, *Electro-Optical Instrumentation: Sensing and Measuring with Lasers* (Prentice Hall, 2004).
14. R. P. Green, J. H. Xu, L. Mahler, A. Tredicucci, F. Beltram, G. Giuliani, H. E. Beere, and D. A. Ritchie, Appl. Phys. Lett. **92**, 071106 (2008).
15. S. Donati, *Photodetectors* (Prentice Hall, 1999).
16. S. Donati and M. Sorel, IEEE Photon. Technol. Lett. **8**, 405 (1996).
17. G. Scalari, L. Ajili, J. Faist, H. Beere, E. H. Linfield, D. Ritchie, and G. Davies, Appl. Phys. Lett. **82**, 3165 (2003).
18. D. Indjin, P. Harrison, R. W. Kelsall, and Z. Ikonic, Appl. Phys. Lett. **82**, 1347 (2003).
19. Y. L. Lim, R. Kliese, K. Bertling, K. Tanimizu, P. A. Jacobs, and A. D. Rakić, Opt. Express **18**, 11720 (2010).
20. S. Barbieri, J. Alton, H. E. Beere, J. Fowler, E. H. Linfield, and D. A. Ritchie, Appl. Phys. Lett. **85**, 1674 (2004).
21. K. Rochford and A. Rose, Opt. Lett. **20**, 2105 (1995).
22. J. R. Tucker, A. D. Rakic, C.J. O'Brien, and A. V. Zvyagin, Appl. Opt. **46**, 611 (2007).